

General Articles

Magnetic resonance imaging of the equine foot: 15 horses

S. DYSON*, R. MURRAY, M. SCHRAMME and M. BRANCH

Centre for Equine Studies, Animal Health Trust, Lanwades Park, Kentford, Newmarket, Suffolk CB8 7UU.

Keywords: horse; MRI; equine foot; lameness; nuclear scintigraphy; deep digital flexor tendonitis; navicular disease

Summary

Reasons for performing study: Foot pain is a common cause of equine lameness and there have been significant limitations of the methods available for the diagnosis of the causes of foot pain (radiography, nuclear scintigraphy and ultrasonography). Until recently, magnetic resonance imaging (MRI) in the horse has been limited to examination of cadaver limbs.

Objectives: Our purpose was to 1) describe MRI of the foot in live horses, 2) describe MRI findings in horses with foot pain in which a definitive diagnosis could not be established by alternative means and 3) correlate MRI findings with other methods of clinical investigation.

Methods: The feet of 15 horses with unilateral (12) or bilateral (3), forelimb (14) or hindlimb (1) lameness associated with foot pain of previously ill-defined origin were examined using MRI. The horses were examined in right lateral recumbency under general anaesthesia, with the feet positioned in the isocentre of a flared end 1.5 Tesla GE Signa EchoSpeed magnet. Images were obtained in sagittal, transverse and dorsal planes using 3-dimensional (3D) T2* gradient echo (GRE), spoiled gradient echo, fat-saturated 3D T2* GRE and short inversion recovery sequences. Image acquisition took approximately 1 h.

Results: Abnormalities of the distal interphalangeal joint (DIP) cartilage and/or subchondral bone, periarticular osteophyte formation, distension of the DIP joint capsule with or without synovial proliferation, distension of the navicular bursa with or without evidence of chronic inflammation, surface and core lesions in the deep digital flexor tendon, abnormal signal within the navicular bone, evidence of mineralised fragments in the distal sesamoidean impar ligament, irregular outline of and signal in the medial cortex of the distal phalanx, and an abnormal signal on the dorsal aspect of the distal phalanx consistent with laminitis were identified.

Conclusions: MRI permits the diagnosis of a variety of lesions involving different structures within the foot that cannot be diagnosed using other means, thus enhancing our knowledge of the causes of foot pain.

Potential relevance: With further experience it is likely that

lesions involving other structures will also be identified. Long-term follow-up data is required to determine the prognosis for the injuries described.

Introduction

Foot pain is a common cause of equine lameness and, although pain is easily localised to the foot, there have been significant limitations of the methods available for the diagnosis of the causes of foot pain. Radiography is limited to the assessment of mineralised tissues and, since images are obtained through the entire thickness of the foot and a 40% change in bone density is required before changes can be identified, small abnormalities are easily missed (Butler *et al.* 2000). Nuclear scintigraphy provides highly sensitive information about abnormal bone activity, but anatomical localisation is limited and there is a relatively high incidence of false positive results (Dyson 2002). Ultrasonography of the foot is limited to the sagittal midline and off incidence artefacts may confuse interpretation (Denoix 2000; Sage and Turner 2000; Busoni and Denoix 2001). Computed tomography (CT) can be used for accurate assessment of the 3-dimensional (3D) distribution of both bone and soft tissue lesions, but requires general anaesthesia (Tietje 1995; Ruohoniemi and Tevahartiala 1999; Tietje *et al.* 2001; Tucker 2001).

Until recently, magnetic resonance imaging (MRI) in the horse has been limited to examination of cadaver limbs. There are a number of reports describing lesions identified using MRI in horses with pain localised to the foot (Denoix *et al.* 1993; Whitton *et al.* 1998; Widmer *et al.* 2000) and a recent detailed study of imaging sequences to examine the osseous and soft tissue structures of the digit (Kleiter *et al.* 1999).

Our purpose was to 1) describe MRI of the foot in live horses, 2) describe MRI findings in horses with foot pain in which a definitive diagnosis could not be established by alternative means and 3) to correlate MRI findings with other methods of clinical investigation.

Materials and methods

For ease of reference, the distal sesamoid bone is referred to as the navicular bone throughout the text.

Fifteen horses with unilateral or bilateral forelimb lameness, or unilateral hindlimb lameness, with pain localised to the foot,

*Author to whom correspondence should be addressed.

TABLE 1: Examples of MR sequences used for imaging feet to show the plane used, time taken for each sequence, slice thickness and field of view used to produce diagnostic images in an average horse

Sequence	Plane	TR (ms)	TE (ms)	FE/PE	NEX	Scan time	Slice thickness (mm)	Interslice spacing (mm)	Field of view (cm)
3 plane localiser	3 plane	135	2.1	256/128	2.0	1 m 47 s	5	1.5	24
3D T2* GRE	Transverse	5.8	1.5	256/192	2.0	2 m 16 s	3	-1.5	22
	Dorsal	5.8	1.5	256/256	2.0	1 m 59 s	3	-1.5	24
	Sagittal	5.8	1.5	256/256	2.0	2 m 05 s	3	-1.5	24
3D T2* GRE fat sat	e.g. Sagittal	15.8	1.5	256/256	2.0	5 m 40 s	3	-1.5	24
3D SPGR	e.g. Sagittal	8.1	3.3	256/256	2.0	2 m 54 s	3	-1.5	24
Fast STIR	e.g. Sagittal	3425	20.0	256/192	1.0	5 m 42 s	4	1.0	22

TR = repetition time; TE = echo time; FE = frequency encoding; PE = phase encoding; NEX = number of excitations; sat = saturated. All 3D sequences used imaging options of variable band width, no phase wrap, extended dynamic range, zero-fill interpolation processing (ZIP 512) to reconstruct the image to a 512/512 matrix, slice ZIP2 - to double the number of reconstructed slices within the prescribed range, representing a location every 1.5 mm (Anon 1999). 2D sequences used variable band width. For the fast STIR sequence, an inversion time of 120 ms and echo train length of 4 were used.

TABLE 2: Age, occupation, lame limb(s), lameness grade and response to local analgesic techniques in 15 horses

Case No.	Age (years)	Occupation	Lame limb(s)	Lameness grade* (lamer limb)	Response to local analgesia of lamer limb			
					PD	P(AS)	DIP	NB
1	14	GP	RF	2-4	S	NP	NP	NP
2	10	SJ	LF>RF	1-2	S	NP	NC	NP
3	7	GP	RF	2-4	NC	S	I (80%)	I (80%)
4	9	GP	RF	4-6	NC	S	I (70%)	NP
5	10	E	LF	4	I (40%)	S	I (80%)	I (95%)
6	8	SJ	RF	1-4	NC	S	I (90%)	NC
7	10	E	LF	2-4	I (60%)	S	NC	S
8	3	R	RF	1-4	S	NP	I (75%)	NP
9	13	SJ	RF>LF	2-4	I (20%)	S	NC	S
10	9	GP	RF	4	S	NP	S	NP
11	15	SJ	LF>RF	1-4	I (20%)	S	I (80%)	NP
12	9	GP	LH	2-4	NP	S	I (75%)	NP
13	9	E	RF>LF	4	I (90%)	S	I (90%)	NP
14	9	E	RF	2-4	I (85%)	S	I (80%)	NC
15	7	GP	LF	4	I (40%)	S	I (40%)	NP

GP = general purpose; SJ = showjumping; E = eventing; R = racing; PD = palmar digital; P(AS) = palmar (abaxial sesamoid); DIP = distal interphalangeal joint; NB = navicular bursa; NP = not performed; NC = no change; I = improved; S = sound. *The range reflects either variability within or between examination periods, or assessment under different circumstances, e.g. straight lines and circles.

were examined using MRI at the Animal Health Trust between January and September 2001. A definitive diagnosis of the cause of pain could not be established using radiography, ultrasonography and, in most horses, nuclear scintigraphy.

All horses were subjected to a detailed clinical examination, with assessment of gait in straight lines on a hard surface and in circles of 10–15 m diameter on both soft and hard surfaces on the lunge. Lameness was graded under each circumstance, on a scale of 0–8 (0 = sound; 2 = mild; 4 = moderate; 6 = severe; 8 = nonweightbearing).

Local analgesic techniques employed included perineural analgesia of the palmar digital nerves and palmar (abaxial sesamoid) nerves (1.5–2.0 ml mepivacaine [Intra-Epicaine]¹/site), intra-articular analgesia of the distal interphalangeal (DIP) joint (6 ml mepivacaine) and intrathecal analgesia of the navicular bursa (3–4 ml mepivacaine), performed under radiographic control. Lameness was reassessed 10 mins after perineural analgesia and 5 mins after intra-articular or intrathecal analgesia. Horses stood still after injection, before re-evaluation of the gait, both in straight lines and circles.

Radiography was performed after removal of the shoes and appropriate preparation of the foot (Butler *et al.* 2000), using lateromedial, dorsoproximal-palmarodistal oblique,

palmaroproximal-palmarodistal oblique views and flexed oblique views of the interphalangeal joints and palmar processes of the distal phalanx.

Ultrasonography of the palmar soft tissues of the pastern was performed using a 10 MHz linear transducer, with and without a stand-off. A 6.5 MHz convex array transducer was used to examine the palmar aspect of the foot via the bulbs of the heel and the centre of the frog.

Nuclear scintigraphy of the feet was performed using vascular, pool and bone phase images and dorsal (or plantar), lateral and solar views were obtained (Dyson *et al.* 2001; Dyson 2002). All horses were lunged for 15 min prior to injection of the radiopharmaceutical (1 GBq/100 kg bwt).

At least 2 weeks elapsed between intrasynovial injections and MRI. Prior to MRI, all shoes were removed and the feet to be examined were cleaned thoroughly. Horses were premedicated with flunixin meglumine (Finadyne Solution)² (0.01 mg/kg bwt) or phenylbutazone (Equipalazone Injection)¹ (0.04 mg/kg bwt) and acepromazine (ACP Injection)³ (0.02 mg/kg bwt). Horses were anaesthetised using romifidine (Sedivet)⁴ or detomidine (Domosedan)⁵ and thiopentone (Thiovet)³ or ketamine (Vetalar V)⁶ and maintained using isoflurane (IsoFlo Vet)² in oxygen. Positive pressure ventilation was used in some horses, but was avoided

TABLE 3: Results of radiographic and nuclear scintigraphic examinations of 15 horses

Case No.	Radiography	Nuclear scintigraphy	
		Pool phase	Bone phase
1	Sole thin; horizontal solar border of distal phalanx	NP	NP
2	Several large lucent zones distal border NB	NAD	LF NB = 103%; RF NB = 116%
3	NAD	RIU in region of DDFT (lateral view)	LF NB = 114%; RF NB = 126%
4	NAD	NP	NP
5	Subtle decrease in corticomedullary demarcation in NB	RIU in region of DDFT (lateral view)	LF NB = 125%
6	NAD	NAD	LF NB = 121%; RF NB = 100%
7	NAD	RIU palmar to NB (lateral view)	Focal RIU lateral palmar process
8	NAD	NP	NP
9	4 large lucent zones distal border NB; mild modelling articular margins DIP joint	RIU palmar to NB (lateral view)	LF NB = 125%; RF NB = 143%
10	NAD	NP	NP
11	Modelling of articular margin of DIP joint	NAD	LF NB = 111%; RF NB = 126%
12	Entheseophyte proximal border NB	NAD	RIU proximolateral aspect of distal phalanx, close to articular margin
13	NAD	RIU region of insertion of DDFT and DSIL (lateral view)	LF NB = 102%; RF NB = 122%
14	Many lucent zones distal and lateral sloping border NB	RIU region of insertion of DDFT and DSIL (lateral view)	LF NB = 100%; RF NB = 121%
15	NAD	RIU insertion of DDFT and DSIL	RIU medial aspect distal phalanx

NAD = no abnormality detected; NB = navicular bone; NP = not performed; RIU = region of increased uptake of radiopharmaceutical. % refers to the ratio of the mean counts per cell in the NB compared to the mean value for the peripheral regions of the distal phalanx measured in solar views (Dyson 2002).

when possible to reduce limb movement. The anaesthetic machine, ventilator and monitoring equipment were nonferrous metal and MR compatible. Each horse was positioned in right lateral recumbency, on a purpose-built, nonferrous metal and glass fibre table of adjustable height. Several people were required to position the limbs to be examined in the isocentre of the short bore, flared end 1.5 Tesla GE Signa Echospeed magnet. A human extremity radiofrequency (RF) coil was placed around the foot to be imaged. Sandbags were placed on the limbs in order to reduce movement associated with respiration.

A 3 plane localiser image was obtained first, to ensure correct positioning of the limbs and for orientation of subsequent sequences. Images were obtained in sagittal, transverse and dorsal planes and included (Table 1) 3D T2* gradient echo (GRE), spoiled gradient echo (SPGR), fat-saturated 3D T2* GRE and short inversion recovery (STIR) sequences (Whitton *et al.* 2003). In some horses, repositioned images were obtained in order to be perpendicular to the most distal part of the deep digital flexor tendon (DDFT). Selection of sequences depended in part on the results of the previous clinical investigations. Both fore feet or both hind feet were examined routinely.

Nuclear scintigraphic images were assessed subjectively and objectively (Dyson 2002). Uptake of the radiopharmaceutical in the navicular bone in solar views was graded as normal (the ratio of uptake in the navicular bone and the peripheral regions of the distal phalanx was <110%), mildly (>110<120%), moderately (>120<140%) or markedly (>140%) increased (Dyson 2002). MR images were analysed and reported by one trained analyst (RM) and verified by the examining clinicians (SD and MS).

Results

Subject details, history and clinical findings are summarised in Table 2. The horses were age 3–14 years and the majority (14) had unilateral (11) or bilateral (3) forelimb lameness. Duration of

lameness varied between 3 and 12 months. All horses underwent radiographic examination and 11 were examined using nuclear scintigraphy. The results are summarised in Table 3.

MRI revealed abnormalities of DIP joint cartilage and or subchondral bone (Figs 1, 2), periarticular osteophyte formation, distension of the DIP joint capsule with or without synovial proliferation (Fig 3), distension of the navicular bursa with or without evidence of chronic inflammation (Fig 4), distension of the digital flexor tendon sheath, surface and core defects in the DDFT (Figs 5, 6), abnormal signal within the navicular bone (Fig 7), evidence of mineralised fragments in the distal sesamoidean impar ligament (DSIL) (Fig 8), irregular outline of and abnormal signal in the medial cortex of the distal phalanx and an abnormal signal on the dorsal aspect of the distal phalanx consistent with laminitis (Fig 9) (Table 4).

Six horses (*Cases 1–6*) had obvious lesions in the DDFT that were restricted to either the medial (2) or lateral (4) lobe. One horse (*Case 2*) with bilateral lameness had bilateral lesions. Three horses (*Cases 1, 5 and 6*) had lesions restricted to the dorsal border of the tendon and the other 3 (*Cases 2, 3 and 4*) had core lesions, one of which also had abnormalities of the dorsal border. The lesions varied in length (1.3–7.0 cm), but usually extended distally from the proximal border of the navicular bursa. One horse (*Case 4*) had a separate lesion in the pastern region that was detectable ultrasonographically. Lameness was eliminated by perineural analgesia of the palmar digital nerves in 2 horses (*Cases 1 and 2*) and was improved in another (*Case 5*). In the remainder, perineural analgesia of the palmar nerves abolished the lameness. Intra-articular analgesia of the DIP joint was performed in 5 of these horses (*Cases 2–6*) and resulted in substantial improvement in 4. Analgesia of the navicular bursa was performed in 3 horses (*Cases 3, 5 and 6*) and produced significant improvement in lameness in 2. No significant radiological abnormality was identified in any of these horses. Ultrasonography failed to identify any of the lesions within the hoof. Nuclear scintigraphic

TABLE 4: Results of magnetic resonance imaging of 15 horses

Case No.	Observations
1	Thin sole and collapsed heels LF and RF. Mineralisation within the cartilage of the medial aspect of the DIP joint, with no evidence of cartilage or subchondral bone roughening. Enlargement of medial branch of DDFT and loss of gap between it and navicular bone; rough dorsal border of DDFT, with a flap displaced dorsally.
2	LF: Linear bright signal in DDFT from proximal limit of navicular bursa to proximal aspect of NB in lateral branch. Dorsal aspect of DDFT roughened. Mild distension DFTS. Distension DIP joint capsule. RF: Bright signal in DDFT and rough dorsal border as LF. Mild distension DFTS.
3	Core lesion in medial branch of DDFT from level of proximal aspect of navicular bursa to distal aspect of NB. Tissue protruding into navicular bursa. Distension of navicular bursa and evidence of chronic inflammation. Roughened medial flexor surface of NB.
4	2 core lesions in lateral branch of DDFT in pastern region; separate core lesions extending from proximal level of navicular bursa to distal aspect of NB. Distension DFTS.
5	Bright signal in NB in fat saturated images. Lesion in dorsal border of lateral branch of DDFT proximal to NB.
6	Lesion in dorsal border of lateral branch of DDFT, extending from proximal aspect of navicular bursa to distal aspect of NB, with dorsopalmar split at level of NB. Bright signal on dorsal aspect of distal phalanx LF and RF.
7	Distension of navicular bursa, with fibrous strands crossing it. Irregular outline of dorsal aspect of DDFT at proximal pouch of navicular bursa. Bright signal in NB in fat saturated images. Mineralisation in DSIL adjacent to midline.
8	Bright signal in NB in central portion. Unusual vasculature medial aspect of NB. Linear increased signal distal border NB laterally.
9	RF. Enlarged navicular bursa with synovial proliferation. Distension and synovial proliferation DIP joint capsule. Osteophyte proximal aspect distal phalanx. Large synovial invaginations distal border NB. Areas of bright signal in NB in fat saturated images. Increased vasculature in NB. LF As above.
10	Rough articular margin of subchondral bone of distal phalanx and defect in subchondral bone margin distal aspect of middle phalanx. Loss of signal in articular cartilage. Mineralisation in DSIL medial to midline.
11	Loss of signal in articular cartilage in DIP joint; irregular outline of cartilage; subchondral bone of distal phalanx irregularly thickened. Synovial proliferation dorsal and palmar pouches DIP joint. Irregular proximal and distal borders of NB. Distension PIP joint capsule RF only.
12	Loss of signal in cartilage lateral aspect of distal phalanx with focal bright signal in subchondral bone overlain by proximal displacement of chondro osseous margin. Irregular distal border NB.
13	Abnormal signal in cartilage lateral aspect of distal phalanx. Bright signal in lateral aspect of NB. Mineralisation in lateral aspect of DSIL, with abnormal fibre pattern in DSIL. Increased fluid in DIP joint and navicular bursa.
14	Areas of fluid accumulation and irregular signal associated with most distal aspect of DDFT and its insertion. Distal border fragments in DSIL on medial and lateral aspects of NB, with associated areas of bright signal in adjacent NB and in body of bone. Similar distal border fragments in LF, but normal NB.
15	Irregular outline of medial cortex of distal phalanx with bright signal in cortical bone. Medial collateral ligament of DIP joint slightly enlarged. Chronic inflammation of DIP joints LF = RF.

No abnormalities were detected in the nonlame limb, unless stated. NB = navicular bone; DFTS = digital flexor tendon sheath; PIP = proximal interphalangeal joint.

examination was performed in 4 horses (*Cases 2, 3, 5 and 6*) and in 2 (*Cases 3 and 5*) there was increased uptake of the radiopharmaceutical in the lateral pool phase image of the lame limb, in the region of the DDFT. Four horses (*Cases 2, 3, 5 and 6*) also had mild or moderately increased uptake of the radiopharmaceutical in the navicular bone of the lame limb, 3 of which had abnormalities of the navicular bone detected using fat-suppressed MR images.

Three horses (*Cases 7–9*) had an abnormally bright signal in the navicular bone in fat-suppressed images as the primary abnormality, in 2 of which there was also marked distension of the navicular bursa (*Cases 7 and 9*). In all 3 horses, lameness was improved or eliminated by perineural analgesia of the palmar digital nerves. Intra-articular analgesia of the DIP joint did not alter the lameness in any horse, but intrathecal analgesia of the navicular bursa removed the lameness in the 2 horses with distension of the navicular bursa. Radiolucent zones along the distal border of the navicular bone were the only radiological observation. Nuclear scintigraphy was performed in 2 horses (*Cases 7 and 9*) and revealed focal increased uptake of the radiopharmaceutical palmar to the navicular bone in the lateral pool images in both horses and markedly and moderately increased uptake in the navicular bone of the lame and less lame limbs in one (*Case 9*). Four additional horses (*Cases 5, 13–15*) with other concurrent abnormalities detected using MRI also had a bright signal within the navicular bone.

Three horses (*Cases 10–12*) had primary abnormalities in the DIP joint, 2 with evidence of osteoarthritis (*Cases 10 and 11*) and the third with a focal bright signal in the subchondral bone of the distal phalanx. One horse also had mineralisation within the DSIL. Lameness was improved by perineural analgesia of the palmar digital nerves in *Case 11* and was eliminated in *Case 10*. Intra-articular analgesia of the DIP joint produced substantial improvement in all horses. Intrathecal analgesia of the navicular bursa had no effect in *Case 11*. One horse (*Case 11*) had radiographic evidence of mild modelling of the articular margins of the DIP joint and another (*Case 12*) had enthesioid bone on the proximal border of the navicular bone. Nuclear scintigraphy revealed moderately increased uptake of the radiopharmaceutical in the navicular bone of the less lame limb and mildly increased uptake in the lame limb in *Case 11*. *Case 12* had a focal region of increased uptake of the radiopharmaceutical in the proximolateral aspect of the distal phalanx, corresponding with the lesion identified using MRI.

Two horses (*Cases 13 and 14*) had several abnormalities in the region of the DSIL and insertion of the DDFT, the navicular bone and the DIP joint. Lameness was substantially improved by perineural analgesia of the palmar digital nerves and abolished by palmar nerve blocks. Intra-articular analgesia of the DIP joint resulted in marked improvement in lameness, but intrathecal analgesia of the navicular bursa, performed only in *Case 14*, did not alter the lameness. Radiography revealed many lucent zones



Fig 1: Sagittal 3D SPGR image of the left front foot of Case 11. The signal in the articular cartilage of the distal interphalangeal joint is heterogeneous and the borders of the cartilage are poorly demarcated. Compare with the proximal interphalangeal joint. The subchondral bone of the distal phalanx is irregular in outline and thickness (arrows). Compare with Figure 3.



Fig 3: Sagittal 3D T2* GRE image of the left front foot. There is distension of the DIP joint capsule with fluid (bright signal) and synovium (lower signal) in the dorsal and palmar pouches (arrows).



Fig 2: Dorsal 3D T2* GRE image of the left hindlimb of Case 12. Lateral is to the right. Lateral to the midline the signal in the articular cartilage is heterogeneous. There is a focal bright signal in the underlying subchondral bone (arrow). The bright signal was not seen in fat-saturated images. The bright signal corresponded with a focal area of increased uptake of radiopharmaceutical.



Fig 4: Sagittal 3D T2* GRE image of the left forelimb of Case 7. The navicular bursa is distended (bright signal) (arrow) and there are fibrinous strands crossing it.

along the distal and lateral sloping borders of the navicular bone in Case 14. Nuclear scintigraphy revealed increased uptake of the radiopharmaceutical in lateral pool phase images of the lateral limb in the region of insertion of the DDFT and DSIL and moderately increased uptake in the navicular bone in bone phase images of both horses.

One horse (Case 15) had an abnormal signal in the cortical bone on the medial aspect of the distal phalanx. Lameness was improved by perineural analgesia of the palmar digital nerves and abolished by palmar nerve blocks. Intra-articular analgesia of the DIP joint resulted in slight improvement. Nuclear scintigraphy revealed increased uptake of the radiopharmaceutical in the medial aspect of the distal phalanx.

Between the initial clinical investigation, including scintigraphy, and MRI, the DIP joint of Case 6 had been

medicated with triamcinolone by the referring veterinary surgeon. Subsequently, the horse had developed signs of laminitis bilaterally and at the time of MRI still had increased sensitivity to hoof tester pressure at the toes, although digital pulse amplitudes were normal, the gait was not typical of laminitis and no radiographic abnormalities were detectable. An abnormal bright signal was identified on the dorsal border of the distal phalanx bilaterally, compatible with laminitis (Murray *et al.* 2003).

Discussion

MRI of live horses is logistically possible and, with a trained team, a straightforward procedure. The shape of the magnet limits examination to the carpus and tarsus and more distal aspects of the limbs and the head. Imaging of both front feet takes approximately



Fig 5a: Sagittal 3D SPGR image of the right forelimb of Case 4. There is a core lesion in the deep digital flexor tendon (bright signal) (arrows) which extended approximately 50 mm proximodistally.



Fig 6: Sagittal 3D T2* GRE fat-suppressed image of the left front foot of Case 5. There is bright signal on the dorsal border of the deep digital flexor tendon (arrow). Transverse images showed that this was restricted to the lateral lobe of the deep digital flexor tendon.



Fig 5b: Transverse 3D T2* GRE image of the right forelimb of Case 4. Lateral is below. There is a core lesion in the lateral lobe of the deep digital flexor tendon. The lateral lobe is enlarged compared to the medial lobe and has an irregular dorsal margin (compare bracketed regions).

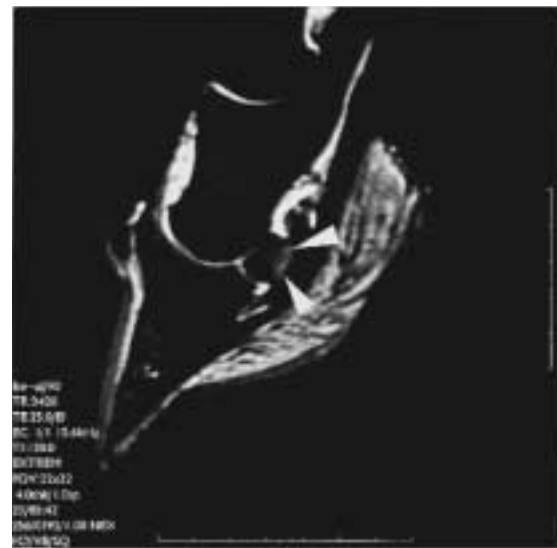


Fig 7: Sagittal 2D STIR image of the left front foot of Case 5. There is a bright signal within the palmar aspect of the medulla of the navicular bone (arrows).

1 h. MRI is not a screening tool and it is essential to be focused, based upon the results of a previous comprehensive clinical investigation, so that examination is limited to a specific region and appropriate imaging sequences are selected based upon the suspected lesion.

MRI has a number of advantages compared to other imaging techniques, including radiography, nuclear scintigraphy, ultrasonography and CT. Unlike radiography and ultrasonography, MRI provides 3D images. The entire foot is accessible and MRI provides physiological information that is anatomically specific, unlike scintigraphy. The technique is adaptable and, therefore, different imaging sequences can be used to target the examination, based on previous information about the potential site of the lesion. The relative merits of CT and MRI in the horse are yet to

be fully determined; however, both require general anaesthesia. CT can be used for assessment of bone and soft tissues and may be more sensitive to changes in bone surface contour than MRI (Whitton *et al.* 1998), although the soft tissue contrast and detection of medullary fluid are inferior to MRI (Whitton *et al.* 1998; Tietje *et al.* 2001) and cartilage can only be evaluated using invasive arthrography. MRI is expensive because of the capital costs of the equipment. Positioning a horse in the magnet is labour-intensive, but image acquisition is not. With both CT and MRI many images are obtained and image analysis is therefore time-consuming and requires experience.

Interpretation of the findings in this study was based on comparison with previous cadaver studies of normal horses (C. Whitton *et al.*, unpublished data) and published normal studies



Fig 8: Dorsal 3D T2* GRE image of a left front foot. Lateral is to the right. There is a focal area of decreased signal in the distal sesamoidean impar ligament laterally (arrows) immediately distal to the navicular bone. The distal border of the navicular bone is rather irregular.

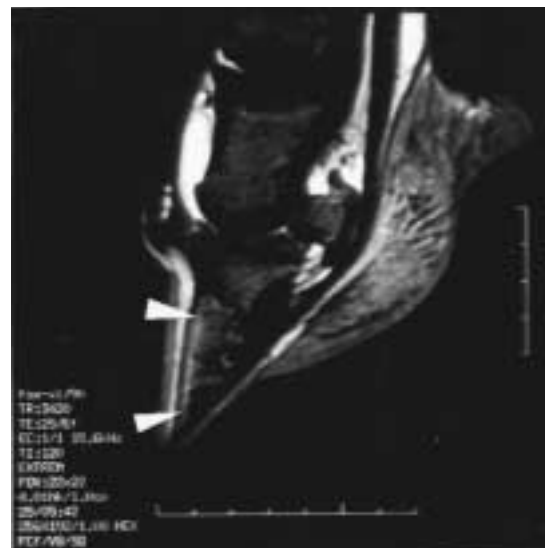


Fig 9: Sagittal 2D STIR image of the right front foot of Case 6. There is a bright signal along the dorsal border of the distal phalanx (arrows). There is also bright signal within the medulla of the navicular bone.

(Park *et al.* 1987; Kleiter *et al.* 1999; Kotani *et al.* 2000) and also with horses with pathological abnormalities of the foot verified at *postmortem* (C. Whitton *et al.*, unpublished data; Murray *et al.* 2003) or recorded previously (Denoix *et al.* 1993; Ruohoniemi *et al.* 1997; Whitton *et al.* 1998; Widmer *et al.* 2000).

The MR pulse sequences used in these horses were based on previous experience with cadaver limbs. GRE and SPGR sequences had the advantages compared to spin echo or fast spin echo sequences of allowing 3D acquisition and a sufficiently high acquisition speed for practical clinical scanning. For high detail, 3D GRE and SPGR sequences with minimal thickness, contiguous slices maximised information obtained in the shortest time. Fat-suppression techniques are used to reduce interference from the fat signal and are particularly useful in detecting bone medullary fluid (Jiang *et al.* 1999). In this case series, fat suppression was of significant benefit in detection of fluid on T2-weighted sequences and in improving subtle T1 contrast between articular cartilage and synovial fluid. The selective chemical (spectral) presaturation technique saturated out purely the fat signal and could be used for 3D imaging, thereby maintaining a high resolution, detailed image. However, as chemical presaturation works best with a uniformly shaped body part, problems did occur in the distal aspect of the limb, where the angular shape sometimes resulted in poor fat saturation and, almost invariably, resulted in inconsistent fat saturation in the proximal phalanx. In contrast, use of the 2D STIR sequence for fat suppression resulted in less detail, but good contrast, with more consistent fat suppression.

Both methods of fat suppression detected fluid signal in the navicular bone and the distal phalanx. For sagittal images of the navicular bone, the STIR sequences showed relatively increased contrast and clearer definition of pathology than fat saturation. However, fat saturation resulted in better detail in transverse images and was better for identification of focal areas of subchondral bone pathology. STIR sequences are time-consuming and it is, therefore, only practical to obtain relatively thick slices, so that focal lesions may be missed.

In human subjects, MRI is currently considered the most

sensitive technique for detecting bone pathology including osteonecrosis, osteomyelitis and trauma, such as bone contusion and undisplaced fractures, as well as articular cartilage pathology and soft tissue lesions (Jiang *et al.* 1999). In the current study, both GRE and SPGR sequences showed clear delineation of bone surface contour and detection of osteophytes, which is in agreement with findings in man, where MRI was better for osteophyte detection than conventional radiography (Abraham-Zadeh *et al.* 1994). In these horses, use of fat suppression improved the contrast at the bone surface in T2-weighted images, but subchondral bone irregularity was seen best on standard images. Using fat-suppressed T2* GRE or STIR images, a fluid signal was detected in the navicular bone, subchondral bone of the DIP joint and the distal phalanx. In man, this fluid signal reflects bone necrosis, inflammation, trabecular microdamage, fibrosis and bone oedema (Rangger *et al.* 1998; Zanetti *et al.* 2000).

We have found fluid signal in the navicular bone at sites with histological evidence of oedema (R. Murray *et al.*, unpublished data) and in the dorsal aspect of the distal phalanx from horses with chronic laminitis (Murray *et al.* 2003). Core lesions of the DDFT were detectable using both T2* GRE and SPGR sequences, but were not obvious using STIR, which is probably related to slice thickness. Dorsal border lesions at the level of the navicular bursa were most obvious on T2* GRE images, largely related to the contrast between the high signal of the synovial fluid and low signal of the tendon. High signal in tendon on both T1- and T2-weighted images has been shown previously to reflect both acute tendonitis and the later phases of healing (Crass *et al.* 1992). Articular cartilage pathology was most evident on fat-suppressed 3D T2* GRE images, as the fat suppression not only improved contrast in the cartilage itself, but also highlighted subtle areas of subchondral bone oedema, which is recognised as potentially indicating a defect in the overlying articular surface (Rubin *et al.* 2000). For accurate cartilage morphological measurements and detection of surface defects, fat-suppressed or standard SPGR imaging is reported to be the technique of choice in man (Disler *et al.* 1995; Cicuttini *et al.* 2000) and, in the current study, this

technique gave high resolution of the articular cartilage and good discrimination from both synovial fluid and subchondral bone.

Although artefacts similar to those reported in human clinical imaging were observed in MR imaging of the equine foot, particular problems were noted. Respiratory motion resulted in significant movement of the upper forelimb, causing motion artefacts. These were most evident on T2* GRE and STIR images and caused less problems on SPGR images. Motion was maximal during positive pressure ventilation and was minimised by spontaneous ventilation and weighting of the limbs with sandbags. Although respiratory triggering techniques were used in some horses, these did not improve the images significantly and prolonged acquisition time. Magnetic susceptibility artefacts were common and generally associated with nail fragments in the feet. T2* GRE images were most vulnerable to magnetic susceptibility effects, as reported in other species (Jiang *et al.* 1999). However, careful shoe removal and cleaning of the foot minimised these artefacts to an acceptable level in all horses. A bright signal in the DDFT was often seen near its insertion, due to the magic angle effect, seen when collagen fibres are located at an angle of 54.7° to the static magnetic field. This was most obvious on SPGR images and less evident on T2-weighted images, where the echo time was longer.

In this series of 15 horses, abnormalities of the DIP joint cartilage and subchondral bone, lesions of the DDFT, abnormalities of the navicular bursa, pathological changes in the navicular bone, abnormal signal in the DSIL and lesions of the distal phalanx consistent with laminitis were identified. There was an interesting correlation with previously performed diagnostic techniques. Of the 6 horses with primary DDFT lesions, 4 of 5 responded to analgesia of the DIP joint and 2 of 3 to analgesia of the navicular bursa, whereas none of the 3 horses with primary navicular bone lesions responded to analgesia of the DIP joint, but both horses in which analgesia of the navicular bursa was performed had a positive response. This study verified the potential sensitivity and usefulness of scintigraphy in localising the anatomical position of the lesions. This required high quality pool and bone phase images, analysed both subjectively and quantitatively, and superimposition of radiographic and scintigraphic images for accurate anatomical localisation of regions of increased uptake of radiopharmaceutical (RIUs).

The majority (6) of DDFT lesions were located proximal to the navicular bone, a region inaccessible for ultrasonographic evaluation via the sole and an area where the ultrasound beam cannot be perpendicular to the line of the fibres if imaging is performed via the heel. Examination via the heel permits some degree of evaluation of the size of the medial and lateral lobes of the navicular bone and dystrophic mineralisation may be seen, but was not present in any of these horses. The lesions were usually restricted to either the medial or lateral lobe of the tendon; therefore, those lesions extending to the level of the navicular bone were not identified by ultrasonographic imaging via the axial midline of the frog. The site of these lesions correlated with the location of an RIU in a lateral pool phase scintigraphic image in 2 of 4 horses. None of these lesions extended to the insertion of the DDFT on the distal phalanx and uptake of radiopharmaceutical in this region in lateral and solar bone phase images was normal. However, 2 horses with MRI abnormalities in the region of insertion of the DDFT and DSIL did have an RIU in this region in lateral pool phase images. Lesions of the DDFT within the hoof capsule have previously been identified *post mortem* (Dyson and Kidd 1993), by bursoscopy of

the navicular bursa (Dyson 1998; S.J. Dyson and C. Whitton, unpublished data) and using CT (M. Nowak, personal communication) but, based on this study and that of M. Nowak (personal communication) it is likely that the incidence has previously been underestimated. Fifteen of 78 horses examined using CT had lesions in the DDFT in the digit, without associated abnormalities of the navicular bone, the most common site for which was proximal to the navicular bone (M. Nowak, personal communication), as in the current study.

The correlation between MRI of acute superficial digital flexor tendon injuries in the metacarpal region and histopathological appearance has been described and lesions of up to 7 weeks duration were readily detectable using MRI (Crass *et al.* 1992). Collagen necrosis, haemorrhage and adjacent chondroid metaplasia were features of DDFT core lesions in 2 horses with lameness of 3 and 6 months duration, respectively, which appeared similar using MRI to the core lesions described in this study (Whitton *et al.* 1998; S.J. Dyson and C. Whitton, unpublished data). Tissue protruding into the navicular bursa has represented fibrillated fibres of the dorsal aspect of the DDFT (C. Whitton *et al.*, unpublished data).

Two horses had MRI evidence of osteoarthritis of the DIP joint, one of which had mild periarticular osteophyte formation detected radiographically. Radiography was an insensitive indicator of pathological abnormalities of the subchondral bone and articular cartilage, which were clearly demonstrated using MRI. There was normal radiopharmaceutical uptake in the region of the DIP joint in both of these horses, but in the horse with a focal bright signal in the subchondral bone of the distal phalanx, compatible with an osseous cyst-like lesion, there was excellent correlation with an RIU.

Distension of the DIP joint capsule was seen frequently and not restricted to the lame limb, but enlargement of the navicular bursa was seen only in the lame limb(s) and was identified in 4 horses (*Cases 3, 7, 9 and 13*). Three of these horses had an RIU palmar to the navicular bone in lateral pool phase images. Distension of the navicular bursa can be identified ultrasonographically via the frog, but only a limited portion can be examined properly. Previously, the only method of verification of navicular bursitis was by invasive bursoscopy, which is a useful diagnostic method and has been used to identify DDFT and DSIL lesions and erosions of the flexor surface of navicular bone (Dyson 1998; S.J. Dyson and C. Whitton, unpublished data). However, examination is limited to the proximal pouch of the bursa and the immediately adjacent structures. Two of the horses in this study (*Cases 7 and 9*) have responded to medication of the navicular bursa.

Although changes in outline of the navicular bone were detected in standard sequences, fat-suppressed images were required to identify changes in internal architecture of the navicular bone, which were identified in 7 horses. Six of these horses were examined scintigraphically and a marked or moderate RIU was identified in the navicular bone in 4. The bright signal in the navicular bone is compatible with bone oedema and we speculate that it might represent venous congestion of marrow spaces. An additional horse with a primary DDFT lesion also had roughening of the medial aspect of the flexor surface of the navicular bone associated with a moderate RIU in the navicular bone.

Areas of low signal in the DSIL compatible with mineralised fragments were identified in 4 horses (*Cases 7, 10, 13 and 14*), the clinical significance of which remains unclear. In one horse (*Case*

14) there were medial and lateral fragments bilaterally but, in the lame limb, there were areas of bright signal in the adjacent navicular bone. None of the fragments were identified radiographically in any horse. The incidence of fragments in the DSIL was higher in a *post mortem* study of horses with navicular disease compared to age-matched controls and many could not be identified radiographically (Wright *et al.* 1998).

The interpretation of the MRI findings in this study must be viewed in light of the other diagnostic information available, since none of the horses was examined *post mortem*. It is hoped that as a result of more accurate identification of the causes of foot pain more appropriate treatment regimes can be developed and, in the future, more accurate prognostic information will be available.

Acknowledgements

We would like to thank Dr Russ Tucker for his invaluable assistance in the preliminary development of imaging sequences, the Animal Health Trust anaesthetists and yard staff and the referring veterinary surgeons. We also thank John Wilkinson for production of the figures.

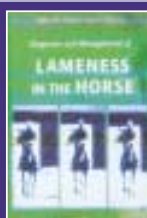
Manufacturers' addresses

- ¹Arnolds Veterinary Products Ltd., Harlescott, Shrewsbury, UK.
²Schering-Plough Animal Health, Uxbridge, Middlesex, UK.
³Vericore, Novartis Animal Health Ltd., Litlington, Hertfordshire, UK.
⁴Boehringer Ingelheim Ltd., Bracknell, Berkshire, UK.
⁵Pfizer Ltd., Sandwich, Kent, UK.
⁶Pharmacia and Upjohn Animal Health Ltd., Corby, Northamptonshire, UK.

References

- Abraham-Zadeh, R., Yu, J. and Resnick, D. (1994) Central (inferior) osteophytes of the distal femur: imaging and pathological findings. *Invest. Radiol.* **29**, 1001-1005.
- Anon (1999) *Signa MR Scan Assistant Manual*, 8.3 Software Release 2148091-100, Revision 3 (6/99), General Electric Company. pp 1-5.
- Busoni, V. and Denoix, J.-M. (2001) Ultrasonography of the podotrochlear apparatus in the horses using a transcuneal approach: technique and reference images. *Vet. Radiol. Ultrasound* **42**, 534-540.
- Butler, J., Colles, C., Dyson, S., Kold, S. and Poulos, P. (2000) The foot, pastern and fetlock. In: *Clinical Radiology of the Horse*, 2nd edn., Blackwell Scientific, Oxford. pp 27-130.
- Cicutini, F., Forbes, A., Asbeutah, A., Morris, K. and Stuckey, S. (2000) Comparison and reproducibility of fast and conventional spoiled gradient echo magnetic resonance sequences in the determination of knee cartilage volume. *J. Orthop. Res.* **18**, 580-584.
- Crass, J., Genovese, R., Render, J. and Bellon, E. (1992) Magnetic resonance, ultrasound and histopathologic correlation of acute and healing tendon injuries. *Vet. Radiol. Ultrasound* **33**, 206-216.
- Denoix, J.-M. (2000) *The Equine Distal Limb: An Atlas of Clinical Anatomy and Comparative Imaging*, Manson Publishing Ltd., London.
- Denoix, J.-M., Crevier, N., Roger, B. and Lebas, J. (1993) Magnetic resonance imaging of the equine foot. *Vet. Radiol. Ultrasound* **34**, 405-411.
- Disler, D., McCauley, T., Wirth, C. and Fuchs, M. (1995) Detection of knee hyaline cartilage defects using fat-suppressed three-dimensional spoiled gradient-echo MR imaging: comparison with standard MR imaging and correlation with arthroscopy. *Am. J. Radiol.* **165**, 377-382.
- Dyson, S. (1998) The puzzle of distal interphalangeal joint pain. *Equine vet. Educ.* **10**, 119-125.
- Dyson, S. (2002) Subjective and quantitative scintigraphic assessment of the equine foot and its relationship with foot pain. *Equine vet. J.* **34**, 164-170.
- Dyson, S. and Kidd, L. (1993) A comparison of responses to analgesia of the navicular bursa and intra-articular analgesia of the distal interphalangeal joint in 59 horses. *Equine vet. J.* **25**, 93-98.
- Dyson, S., Lakhani, K. and Wood, J. (2001) Factors influencing blood flow in the equine digit and their effect on uptake of ^{99m}technetium methylene diphosphonate into bone. *Equine vet. J.* **33**, 591-598.
- Jiang, Y., Peterfly, C., Zhao, J., White, D., Lynch, J. and Genant, H. (1999) Magnetic resonance imaging in osteoarthritis. In: *Osteoarthritis. Clinical and Experimental Aspects*, Eds: J.Y. Reginster, J.P. Pelletier, J. Martel-Pelletier and Y. Henrotin, Springer-Verlag, New York. pp 268-295.
- Kleiter, M., Kneissl, S., Stanek, C., Mayrhofer, E., Baulain, U. and Deegan, E. (1999) Evaluation of magnetic resonance imaging techniques in the equine digit. *Vet. Radiol. Ultrasound* **40**, 15-22.
- Kotani, H., Taura, Y., Sakai, A., Tsuka, T. and Kageyama, Y. (2000) *Antemortem* evaluation of magnetic resonance imaging of the equine flexor tendon. *J. vet. Med. Sci.* **62**, 81-84.
- Murray, R., Dyson, S., Schramme, M., Branch, M. and Woods, S. (2003) Magnetic resonance imaging of chronic laminitis. *Vet. Radiol. Ultrasound*. In press.
- Park, R., Nelson, T. and Hoopes, P. (1987) Magnetic resonance imaging of the normal equine digit and metacarpophalangeal joint. *Vet. Radiol.* **28**, 105-116.
- Ranger, C., Kathrein, A., Freund, M., Klestil, T. and Kreczy, A. (1998) Bone bruise of the knee. Histology and cryosections in 5 cases. *Acta Orthop. Scand.* **69**, 291-294.
- Rubin, D., Harner, C. and Costello, J. (2000) Treatable chondral injuries in the knee: frequency of associated focal subchondral edema. *Am. J. Roentgenol.* **174**, 1099-1106.
- Ruohoniemi, M. and Tevahartiala, P. (1999) Computed tomographic evaluation of Finnhorse cadaver feet with radiographically problematic findings on the flexor surface of the navicular bone. *Vet. Radiol. Ultrasound* **40**, 225-281.
- Ruohoniemi, M., Karkkainen, M. and Tervahartiala, P. (1997) Evaluation of the variably ossified collateral cartilages of the distal phalanx and adjacent anatomical structures in the Finnhorse with computed tomography and magnetic resonance imaging. *Vet. Radiol. Ultrasound* **38**, 344-351.
- Sage, A. and Turner, A. (2000) Ultrasonography in the horses with palmar foot pain: 13 cases. *Proc. Am. Ass. equine Practns.* **46**, 380-381.
- Tietje, S. (1995) Computed tomography of the navicular bone region in the horse: a comparison with radiographic documentation. *Pferdeheilkunde* **11**, 51-62.
- Tietje, S., Nowak, M., Petzoldt, S. and Weiler, H. (2001) Computed tomographic evaluation of the distal aspect of the deep digital flexor tendon (DDFT) in horses. *Pferdeheilkunde* **17**, 21-29.
- Tucker, R. (2001) Computed tomography and magnetic resonance imaging in equine musculoskeletal conditions. *Vet. Clin. N. Am.: Equine Pract.* **17**, 145-157.
- Whitton, C., Murray, R. and Dyson, S. (2003) Magnetic resonance imaging. In: *Diagnosis and Management of Lameness in the Horse*, Eds: M. Ross and S. Dyson, W.B. Saunders Co., Philadelphia. pp 216-222.
- Whitton, C., Buckley, C., Donovan, T., Wales, A. and Dennis, R. (1998) The diagnosis of lameness associated with distal limb pathology in a horse: a comparison of radiography, computed tomography and magnetic resonance imaging. *Vet. J.* **155**, 223-229.
- Widmer, A., Buckwater, K., Fessler, J., Hill, M., Van Sickle, D. and Ivancevich, S. (2000) Use of radiography, computed tomography and magnetic resonance imaging for evaluation of navicular syndrome in the horse. *Vet. Radiol. Ultrasound* **41**, 108-116.
- Wright, I., Kidd, L. and Thorp, B. (1998) Gross, histological and histomorphometric features of the navicular bone and related structures in the horse. *Equine vet. J.* **30**, 220-234.
- Zanetti, M., Bruder, E., Romero, J. and Hodler, J. (2000) Bone marrow edema pattern in osteoarthritic knees: correlation between MR imaging and histologic findings. *Radiol.* **215**, 835-840.

► ORDER ONLINE FROM OUR BOOKSHOP NOW! ◀



DIAGNOSIS AND MANAGEMENT OF EQUINE LAMENESS

Mike W. Ross and Sue J. Dyson

Hardback, 1100 pages,
850 illustrations
Published by Saunders
£110.00 (includes CD-ROM)

This book provides a comprehensive approach to lameness diagnosis and focuses on the importance of clinical examinations and diagnostic analgesia. Detailed descriptions of diagnosis include the common problem of what to do when a diagnosis cannot be made. Musculoskeletal dysfunction is discussed as a cause of poor performance and the management of a broad range of conditions causing gait abnormalities are included.